Annals of Botany **116**: 555–569, 2015
doi:10.1093/aob/mcv122, available online at www.aob.oxfordjournals.org

ANNALS OF BOTANY
Founded 1887

PART OF A SPECIAL ISSUE ON REACTIVE OXYGEN AND NITROGEN SPECIES

Importance of the alternative oxidase (AOX) pathway in regulating cellular redox and ROS homeostasis to optimize photosynthesis during restriction of the cytochrome oxidase pathway in *Arabidopsis thaliana*

Abhaypratap Vishwakarma[1], Sarada Devi Tetali[1], Jennifer Selinski[2], Renate Scheibe[2] and Kollipara Padmasree[3,*]

[1]Department of Plant Sciences, School of Life Sciences, University of Hyderabad, Hyderabad 500 046, India, [2]Department of Plant Physiology, FB5, University of Osnabrück, 49069 Osnabrück, Germany and [3]Department of Biotechnology and Bioinformatics, University of Hyderabad, Hyderabad 500 046, India
** For correspondence. E-mail kpssl@uohyd.ac.in*

Received: 31 January 2015 Returned for revision: 13 March 2015 Accepted: 8 June 2015 Published electronically: 20 August 2015

• **Background and Aims** The importance of the alternative oxidase (AOX) pathway, particularly AOX1A, in optimizing photosynthesis during de-etiolation, under elevated CO_2, low temperature, high light or combined light and drought stress is well documented. In the present study, the role of AOX1A in optimizing photosynthesis was investigated when electron transport through the cytochrome c oxidase (COX) pathway was restricted at complex III.
• **Methods** Leaf discs of wild-type (WT) and *aox1a* knock-out mutants of *Arabidopsis thaliana* were treated with antimycin A (AA) under growth-light conditions. To identify the impact of AOX1A deficiency in optimizing photosynthesis, respiratory O_2 uptake and photosynthesis-related parameters were measured along with changes in redox couples, reactive oxygen species (ROS), lipid peroxidation and expression levels of genes related to respiration, the malate valve and the antioxidative system.
• **Key Results** In the absence of AA, *aox1a* knock-out mutants did not show any difference in physiological, biochemical or molecular parameters compared with WT. However, after AA treatment, *aox1a* plants showed a significant reduction in both respiratory O_2 uptake and $NaHCO_3$-dependent O_2 evolution. Chlorophyll fluorescence and P700 studies revealed that in contrast to WT, *aox1a* knock-out plants were incapable of maintaining electron flow in the chloroplastic electron transport chain, and thereby inefficient heat dissipation (low non-photochemical quenching) was observed. Furthermore, *aox1a* mutants exhibited significant disturbances in cellular redox couples of NAD(P)H and ascorbate (Asc) and consequently accumulation of ROS and malondialdehyde (MDA) content. By contrast, WT plants showed a significant increase in transcript levels of *CSD1, CAT1, sAPX, COX15* and *AOX1A* in contrast to *aox1a* mutants.
• **Conclusions** These results suggest that AOX1A plays a significant role in sustaining the chloroplastic redox state and energization to optimize photosynthesis by regulating cellular redox homeostasis and ROS generation when electron transport through the COX pathway is disturbed at complex III.

Key words: Alternative oxidase pathway, AOX, antimycin A, antioxidants, *Arabidopsis thaliana*, non-photochemical quenching, NPQ, photosynthesis, redox, respiration, reactive oxygen species, ROS.

INTRODUCTION

The mitochondrial electron transport chain (mETC) of higher plants has unique features to transport electrons from reduced ubiquinone to molecular oxygen through the cyanide-insensitive alternative oxidase (AOX) pathway in parallel with the common cyanide-sensitive cytochrome c oxidase (COX) pathway. Electron flow through the COX pathway generates an electrochemical proton gradient across the inner mitochondrial membrane which drives the ATP synthase to convert ADP to ATP. By contrast, electron flow through the AOX pathway is non-phosphorylating as it bypasses two proton translocating complexes and the energy is dissipated as heat (Siedow and Umbach, 2000; Millenaar and Lambers, 2003). Thus, the AOX pathway may appear to be a wasteful process, but based on cellular energy demand, the COX and AOX pathways together maintain the cellular energy balance by regulating their relative distribution.

The role of the AOX pathway in heat generation in thermogenic plants to attract insects as pollinators was identified by Meeuse (1975) and later its significance in floral development was recognized (Wagner *et al*., 2008; Miller *et al*., 2011). Furthermore, its engagement was demonstrated in growth and development of higher plants including *Salsola divaricata*, a C_3–C_4 intermediate plant (Feng *et al*., 2007; Gandin *et al*., 2014*b*; Garmash *et al*., 2015). In addition, the role of AOX has become evident in various biotic and abiotic stress conditions such as combat against bacterial pathogens (Cvetkovska and Vanlerberghe, 2012), low oxygen (Clifton *et al*., 2005), ozone (Tosti *et al*., 2006), nutrient limitation (Noguchi and Terashima, 2006), salinity (Wang *et al*., 2010), metal toxicity

(Tan *et al*., 2010), high/low temperature (Murakami and Toriyama, 2008; Wang *et al*., 2011), high light (HL) and/or drought (Giraud *et al*., 2008; Vassileva *et al*., 2009; Zhang *et al*., 2010; Yoshida *et al*., 2011*a*; Zhang *et al*., 2012) and high CO_2 (Gandin *et al*., 2012).

Under abiotic stress conditions, the contribution of AOX-catalysed respiration becomes significant. It dissipates excess energy in the form of heat and thereby prevents over-reduction of the ubiquinone (UQ) pool, which in turn inhibits the generation of reactive oxygen species (ROS) (Vassileva *et al*., 2009; Yoshida *et al*., 2011*a*). The role of AOX is also recognized in alleviation of reactive nitrogen species, particularly of NO levels in mitochondria, which are induced by reducing equivalents (Gupta *et al*., 2012; Cvetkovska *et al*., 2014; Igamberdiev *et al*., 2014). The role of AOX is not limited to combating stress and was also proposed to be triggered by a variety of signals and acts as a buffer which determines the threshold for the induction of programmed cell death (Van Aken *et al*., 2009). In breeding studies, AOX was suggested as a marker to bring about efficient cell reprogramming during growth and development under stressful conditions (Arnholdt-Schmitt *et al*., 2006).

In addition, the physiological role of AOX is well accepted in optimizing photosynthesis. Several studies have demonstrated that any interference in the COX or AOX pathway (using mutants or chemicals) caused a significant decrease in photosynthetic O_2 evolution in mesophyll protoplasts or leaf tissue (Padmasree and Raghavendra, 1999*a*; Yoshida *et al*., 2006; Strodtkötter *et al*., 2009; Dinakar *et al*., 2010*a*; Zhang *et al*., 2012; Vishwakarma *et al*., 2014). However, during stress conditions (drought, HL, high CO_2 and temperature) engagement of the AOX pathway was much higher compared with the COX pathway (Vassileva *et al*., 2009; Dinakar *et al*., 2010*b*; Gandin *et al*., 2012, 2014*b*; Zhang *et al*., 2014).

During photosynthesis, reducing equivalents are generated via photoreduction of $NADP^+$ catalysed by the ferredoxin-$NADP^+$ reductase (FNR). The regeneration of $NADP^+$, the terminal electron acceptor, is essential for the avoidance of ROS production, otherwise this can lead to damage of the thylakoid membrane (Niyogi, 1999; Raghavendra and Padmasree, 2003). CO_2 assimilation in the Calvin cycle and the malate valve along with malate dehydrogenase (MDH) are essential in $NADP^+$ regeneration, allowing for continued ATP production via the photosynthetic electron transport chain.

Given that plant membranes are broadly impermeable to $NAD(P)^+$ and NAD(P)H, plant cells possess specific translocators enabling the direct and indirect exchange of reducing equivalents. On the one hand, $NAD(P)^+$ can directly be shuttled between subcellular compartments via NAD^+-carrier proteins localized in mitochondria as well as in plastids. However, these transporters exhibit a low affinity for NADH and NADPH (Palmieri *et al*., 2009). On the other hand, plant cells possess specific translocators for the exchange of malate and oxaloacetate (malate–OAA shuttle) enabling the indirect transport of reducing equivalents between different subcellular compartments. Accordingly, malate–OAA shuttles together with MDHs (malate valve) act as a powerful system for balancing the ATP/NAD(P)H ratio and maintaining redox homeostasis in plant cells.

The chloroplastic NADP-dependent MDH (NADP-MDH) uses excess NADPH generated via the photosynthetic electron transport chain to convert OAA to malate, regenerating the electron acceptor $NADP^+$ (Scheibe, 2004). The resulting malate generated through the activity of NADP-MDH in chloroplasts is subsequently translocated to the cytosol via the malate–OAA shuttle, where the interconversion of malate to OAA with concomitant reduction of NAD^+ to NADH catalysed by the redox-regulated cytosolic NAD-dependent MDH takes place (Hara *et al*., 2006). This mechanism allows chloroplastic reducing equivalents to be indirectly transferred to the cytosol and other subcellular compartments, for instance mitochondria, to avoid (1) imbalances in the generation and utilization of reducing equivalents by photochemical reactions and the Calvin cycle and (2) depletion of chloroplast energy carriers which would lead to oxidative stress. A concomitant rise in AOX protein and its respiratory capacity in parallel with an increase in the activity of various enzymes (NADP-malate dehydrogenase, NAD-malate dehydrogenase, NAD-malic enzyme, NADP-isocitrate dehydrogenase) involved in the transport of these reducing equivalents suggests a role of AOX in modulating the cellular redox state and thereby the photosynthetic performances under HL conditions (Fernie *et al*., 2004; Scheibe *et al*., 2005; Yoshida *et al*., 2007, 2008; Xu *et al*., 2011). The rise in cellular levels of pyruvate under HL conditions emphasized the role of AOX in dissipating excess chloroplastic reducing equivalents (Dinakar *et al*., 2010*b*). Thus, the function of AOX is tightly coupled with photosynthesis, as it has a direct impact on the supply and demand of ATP, NAD(P)H and carbon intermediates (Vanlerberghe, 2013). Cooperation between the AOX pathway and NO_3^- assimilation to maintain optimal rates of photosynthesis by regulating the accumulation of reducing equivalents and the over-reduction of the chloroplastic electron transport chain was shown using T-DNA insertion mutants for AOX1A (Gandin *et al*., 2014*a*). The co-expression of *AOX* with other non-phosphorylating genes of the mitochondrial electron transport chain such as *NDB52*, *UCP1* and *UCP2* is well known under HL treatment to prevent an over-reduction of the plastoquinone (PQ) and UQ pools (Yoshida *et al*., 2008, 2011*a*).

In higher plants, *AOX* is encoded by two discrete subfamilies. *AOX1* is widely known to be induced by stress stimuli and is present in both monocot and dicot plants. By contrast, *AOX2* is developmentally expressed and confined to eudicots (Considine *et al*., 2002). In Arabidopsis, *AOX1A* and *AOX1D* are highly stress-responsive amongst hundreds of known genes encoding mitochondrial proteins (Clifton *et al*., 2006), indicating the essentiality of these genes to cope with stress conditions.

Apart from mitochondrial respiration, plants possess several strategies such as photorespiration and antioxidative systems to adapt to stress conditions. Interestingly, these metabolic pathways were found to be modulated upon constraints at AOX (Strodtkötter *et al*., 2009; Voss *et al*., 2013; Vishwakarma *et al*., 2014). Ascorbate (Asc) is an antioxidant molecule which is abundantly present in all subcellular compartments of plant tissues and occurs at as high as 20 mM in chloroplasts (Smirnoff and Wheeler, 2000). It plays an important role in the detoxification of H_2O_2 during stress conditions. Furthermore, *AOX1A* overexpression lines showed higher rates of Asc production when compared with wild-type (WT) in Arabidopsis leaves (Bartoli *et al*., 2006). Various mitochondrial retrograde regulation (MRR) signals are known to stimulate the expression of

AOX1A (Rhoads and Subbaiah, 2007; Suzuki *et al*., 2012). In rice, *AOX1A* and *AOX1B* were expressed during abiotic stress conditions through MRR signalling mediated by O_2^- radicals (Li *et al*., 2013). The deficiency of AOX1A during the restriction of the COX pathway caused a significant reduction in photosynthesis, increase in ion leakage and ROS generation, which ultimately led to wilting and necrosis of the plant in spite of the increase in photorespiration (Strodtkötter *et al*., 2009; Voss *et al*., 2013).

In the present study, we used both chemical and reverse genetic approaches together to examine (1) the physiological importance of AOX1A in modulating the redox state of chloroplastic electron transport carriers and non-photochemical quenching (NPQ) to sustain photosynthesis, and (2) the impact of AOX1A in regulating the malate valve and the antioxidative systems to maintain the cellular redox state and ROS for optimal photosynthetic performance when complex III of the COX pathway is not functional in the presence of antimycin A (AA).

MATERIALS AND METHODS

Plant materials and growth conditions

All experiments were conducted using Columbia (WT) and *aox1a* T-DNA-insertion (SALK_084897) lines of *Arabidopsis thaliana*. We have previously shown that the T-DNA-insertion lines were homozygous for *AOX1A* through northern blot (Strodtkötter *et al*., 2009) and RT-PCR analysis (Vishwakarma *et al*., 2014). Seeds were sown on soilrite mix with half-strength Murashige and Skoog medium (MS medium), followed by stratification at 2–4 °C in the dark for 3–4 d before transferring them to the growth chamber. Plants were watered on alternate days and half-strength MS medium was given twice a week. The plants were maintained in a growth chamber at 22–24 °C with 8-h photoperiod and photosynthetic photon flux density (PPFD) of 50–60 µmol photons m^{-2} s^{-1}.

Antimycin A treatment

Leaf discs (approx. 0·25 cm^2) were prepared from the leaves of 10- to 12-week-old plants with a sharp paper punch under water from either side of the midrib. Leaf discs were placed in a series of Petri dishes containing different concentrations (5, 10, 20, 30 and 40 µM) of AA in 0·01 % Tween-20 and were illuminated for 6 h at 50 µmol photons m^{-2} s^{-1} (growth light). Controls were treated with only 0·01 % Tween-20 in water, but the effect was negligible. The treated leaf discs were directly used to monitor changes in respiration, photosynthesis, chlorophyll fluorescence and ROS levels. Leaf discs were frozen at −80 °C and subsequently analysed for non-protein redox couples (NADH, NADPH and Asc), malondialdehyde (MDA) content and transcript levels.

Measurement of respiration and photosynthesis

The rates of respiratory O_2 uptake and photosynthetic O_2 evolution of leaf discs were monitored using a Clark-type oxygen electrode (LD-2, Hansatech Instruments, King's Lynn, UK). Twenty leaf discs were placed on a topmost nylon mesh, which was homogeneously sprinkled with 200 µL 1·0 M bicarbonate buffer (pH 9·0) to generate approx. 5 % (v/v) CO_2 in the electrode chamber (Walker and Walker, 1987). The levels of O_2 in the electrode chamber were calibrated as per the manufacturer's instructions before measurement of respiratory and photosynthetic rates for each sample. After calibration, the traces of O_2 uptake were monitored for 5 min in the dark and subsequently the traces of O_2 evolution were monitored for 10 min at a PPFD of 250 µmol photons m^{-2} s^{-1}, which is optimal for *A. thaliana* leaves (Vishwakarma *et al*., 2014).

Chlorophyll fluorescence and P700 measurement

Chlorophyll fluorescence and P700 absorbance were measured with a pulse amplitude modulation (PAM) fluorometer (Dual-PAM-100, Heinz Walz GmbH, Effeltrich, Germany). After treatment with AA (20 µM) in the light, the leaf discs were incubated in the dark for 30 min to allow all reaction centres to attain their oxidized state. Chlorophyll fluorescence and P700 parameters were measured for 5 min at 25 °C using the repetitive saturation pulse (SP) method as described by Vishwakarma *et al*. (2014). The intensity and duration of the SP were 3000 µmol photons m^{-2} s^{-1} and 800 ms, respectively. Actinic light (AL) was maintained at 126 µmol photons m^{-2} s^{-1}. The P700-redox state was measured at two different wavelengths (875 and 830 nm) as described by Klughammer and Schreiber (2008). Maximal quantum yield of photosystem II (PSII) (F_v/F_m), effective quantum yield of PSII [Y(II)], photochemical quenching (q*P*), NPQ, electron transport rate of PSII [ETR(II)], quantum yield of PSI [Y(I)], reduced P700 ($P700_{red}$), acceptor-side limitation [Y(NA)] and donor-side limitation [Y(ND)] were automatically calculated by the Dual-PAM-100 software.

NAD(H) and NADP(H) measurements

The total cellular pools of NAD(H) and NADP(H) were measured according to Queval and Noctor (2007). The reduced and oxidized forms of pyridine nucleotides are distinguished by preferential destruction in acid/base. Therefore, leaf discs (100 mg) were finely ground in liquid nitrogen and extracted either in 1·0 mL of 0·2 M HCl for measuring NAD^+ and $NADP^+$ or 0·2 M NaOH for measuring NADH and NADPH, respectively. Pyridine nucleotides were quantified by monitoring the phenazine methosulfate-catalysed reduction of dichlorophenolindophenol. For the assay of NAD^+ and NADH, the reaction was started by the addition of ethanol in the presence of alcohol dehydrogenase. Similarly, for the assay of $NADP^+$ and NADPH, the reaction was started by addition of glucose 6-phosphate dehydrogenase in the presence of glucose 6-phosphate. In both cases, the decrease in A_{600} was monitored for 3 min, and concentrations of the corresponding pyridine nucleotides were calculated from calibration curves with the relevant standards (0–40 pmol).

Measurement of ascorbate and dehydroascorbate levels

Asc and dehydroascorbate (DHA) contents were measured according to Foyer *et al*. (1983). Leaf discs (150 mg) were

ground in 3 mL of 2·5 M $HClO_4$ on ice using a mortar and pestle. The extract was adjusted to pH 5·6 by stepwise addition of 1·25 M K_2CO_3. The resulting precipitate was removed by centrifugation at 8000 *g* for 10 min at 4 °C. The supernatant was used to estimate the Asc and DHA content and Asc/DHA. An aliquot of 100 µL of the supernatant was added to 900 µL of 0·1 M sodium phosphate buffer (pH 5·6) and the absorbance was measured at 265 nm (A). Ascorbate oxidase (2·5 U, Roche Applied Science, Mannheim, Germany) was added to the above mixture and the absorbance at 265 nm was measured (B). A fresh aliquot containing 100 µL of supernatant was incubated with 10 mM reduced glutathione prepared in 0·1 M Tricine–KOH buffer (pH 8·5) for 15 min at room temperature. The volume was then filled up to 1 mL with 0·1 M sodium phosphate buffer (pH 5·6) and the absorbance was measured at 265 nm (C). Asc was measured as the difference of A minus B, while DHA was measured as the difference of C minus A.

Detection of ROS

After AA treatment, leaf discs were vacuum-infiltrated with 25 µM 2,7-dichlorofluorescein diacetate (H_2DCF-DA) at pH 7·4 in 10 mM Tris-HCl (Vishwakarma *et al*., 2014). The non-polar H_2DCF-DA is converted to membrane-impermeable polar H_2DCF by cellular esterases and is rapidly oxidized to highly fluorescent DCF by intracellular H_2O_2. Excess H_2DCF-DA was removed by repeated washing steps of the leaf discs, and the samples were immediately monitored for ROS under a laser-scanning confocal microscope (TCSSP-2, AOBS 4 channel UV and visible; Leica, Wetzlar, Germany) at λ_{ex} 488 nm and λ_{em} 525 nm. Total cellular ROS was monitored as green DCF fluorescence, whereas chloroplastic ROS was detected as orange–yellow fluorescence which is formed due to superimposition of chlorophyll autofluorescence (red) and DCF fluorescence (green).

Measurement of H_2O_2 and lipid peroxidation

Leaf tissue (100 mg) was homogenized in 0·1 % trichloroacetic acid (TCA) on ice. The homogenate was centrifuged at 12 000 *g* for 15 min at 4 °C. The supernatant obtained was used for quantification of both H_2O_2 and lipid peroxidation. Total cellular H_2O_2 was estimated according to Velikova *et al*. (2000), while lipid peroxidation was quantified in terms of MDA content according to Heath and Packer (1968). For the assay of H_2O_2, the supernatant (250 µL) was added to an assay medium containing 250 µL 10 mM potassium phosphate buffer (pH 7·0) and 500 µL 1·0 M KI. Absorbance was measured immediately at 390 nm and the concentration of H_2O_2 was calculated using the relevant standard (0–100 µmol H_2O_2). For the assay of lipid peroxidation, 1·5 mL 20 % TCA containing 0·5 % thiobarbituric acid (TBA) was added to 500 µL supernatant and boiled in a water bath for 30 min. The reaction was stopped by chilling and centrifuged for 5 min at 12 000 *g* at 4 °C. The absorbance of the supernatant was measured at 532 nm and corrected for non-specific absorbance at 600 nm. The MDA content was calculated using the extinction coefficient of the MDA–TBA complex ($\varepsilon = 155\ mM^{-1}\ cm^{-1}$).

RNA isolation and quantitative real-time PCR (qRT-PCR)

Total RNA was extracted from leaf discs using TRI Reagent (Sigma-Aldrich, St Louis, MO, USA) according to the manufacturer's instructions. One microgram of total RNA was used for first-strand cDNA synthesis using the iScript™ cDNA synthesis kit (BioRad, Hercules, CA, USA), which was performed as indicated in the manufacturer's instructions. Transcript levels were measured using a 7500 fast real-time PCR machine (Applied Biosystems, Foster City, CA, USA). Two microlitres of cDNA (50 ng) was amplified in the presence of 10 µL 2× SYBR Green PCR Master Mix (Takara Bio, Shiga, Japan), 0·5 µL specific primers (1·0 pM) and 7·0 µL of sterilized water. PCR conditions were 95 °C for 10 min, 40 cycles of 95 °C for 15 s followed by 60 °C for 1 min. The primers used in the present study are listed in Supplementary Data Table S1. Cycle threshold (C_T) values were obtained from the exponential phase of PCR amplification. The comparative C_T method was used to analyse the relative mRNA expression as described by Livak and Schmittgen (2001). In this method, genes of interest (GOI) were normalized against *UBQ5* (housekeeping gene) expression, generating a ΔC_T value (ΔC_T = GOI C_T − *UBQ5* C_T). The relative expression was then calculated according to the equation $2^{-\Delta\Delta CT}$ and WT without AA was used as a calibrator.

Statistical analysis

Data presented are means (±s.e.) from three to four independent experiments conducted on different days. Triplicates were run in each independent experiment. The differences between treatments were analysed by one-way ANOVA and Tukey's test of multiple comparison analysis using Sigma Plot 11.0 software (San José, CA, USA).

RESULTS

*Effect of AA on total respiratory O_2 uptake and photosynthetic O_2 evolution in WT plants and AOX1A T-DNA mutants (*aox1a*)*

The rates of total respiratory O_2 uptake and bicarbonate-dependent photosynthetic O_2 evolution, the latter an indicator of photosynthetic carbon assimilation (Calvin cycle activity), were monitored in leaf discs of WT and *aox1a* mutants in the presence of AA, a metabolic inhibitor of complex III, to examine the significance of the AOX pathway in optimizing photosynthesis. The inhibition of electron transport through the COX pathway simulates a metabolic state of oxidative stress. In controls, the rates of respiratory O_2 uptake and photosynthetic O_2 evolution varied marginally between WT and *aox1a* mutants. However, the rates of respiratory O_2 uptake and photosynthetic O_2 evolution varied significantly between WT and *aox1a* plants when the leaf discs were exposed to increasing concentrations of AA (Fig. 1A, B). When the concentration of AA was increased from zero to 40 µM, WT leaf discs showed 54 % inhibition in rates of respiratory O_2 uptake and 60 % inhibition in rates of photosynthetic O_2 evolution when compared with their controls without AA. In contrast to WT, in the presence of 40 µM AA, *aox1a* mutants showed 84 % inhibition in rates of respiratory O_2 uptake and 81 % inhibition in rates of photosynthetic O_2 evolution. Thus, these results suggest that

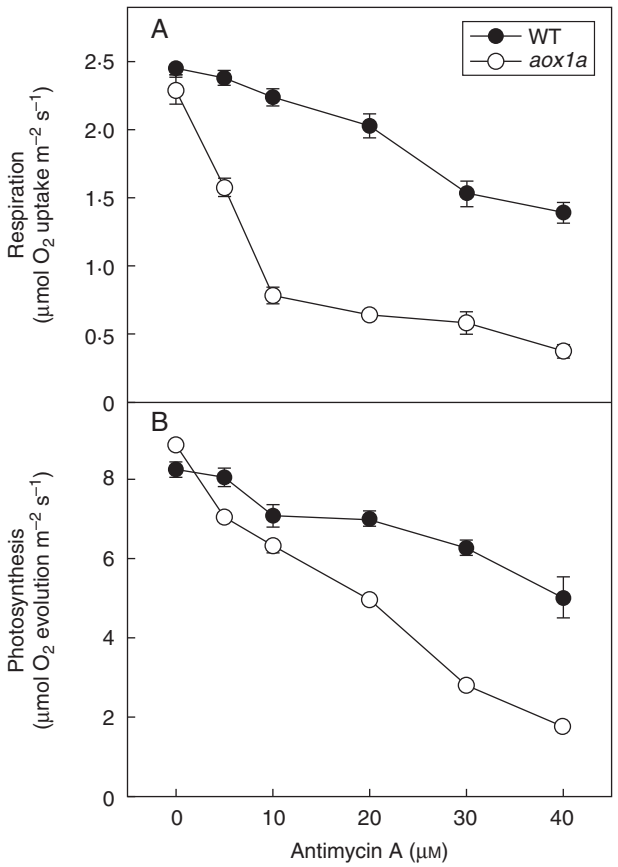

FIG. 1. The rates of respiratory O_2 uptake (A) and photosynthetic O_2 evolution (B) in leaf discs of WT and *aox1a* mutants after pre-illumination (6 h) at a PPFD of 50 μmol m^{-2} s^{-1} at 25 °C in the absence and presence of AA. After pre-illumination, leaf discs were incubated in the dark for 10–15 min during electrode calibration. Subsequently, respiration was measured in the dark for 5 min followed by photosynthesis measured in the light for 10 min at 250 μmol m^{-2} s^{-1} as $NaHCO_3$-dependent (approx. 5 %, v/v) O_2 evolution.

disturbances in the mitochondrial electron transport through the COX pathway compromised the photosynthetic carbon assimilation of chloroplasts more seriously in *aox1a* than in WT. As AA is also known to inhibit cyclic electron transport, a low concentration of AA (20 μM) was used in further experiments. At this concentration, AA caused marginal decreases in rates of respiration and photosynthesis in WT, while the rates of respiration and photosynthesis were drastically reduced in *aox1a* mutants (Fig. 1A, B). These results suggest that 20 μM AA can be applied for restriction of the COX pathway to reveal the importance of AOX1A in optimizing photosynthetic carbon assimilation.

Effect of AOX1A deficiency on chlorophyll fluorescence and P700 parameters in the presence of AA

The changes occurring in chloroplastic reaction centres and the electron transport chain were monitored to examine the importance of AOX1A in keeping up photochemical reactions and thermal dissipation, which play significant roles in photoprotection and meeting the energy demands of the photosynthetic carbon reduction cycle during oxidative stress due to restriction of electron transport through the COX pathway. The maximum quantum yield of PSII (F_v/F_m), which indicates the maximum efficiency of PSII, was measured after applying the initial SP. In the absence of AA, both WT and *aox1a* knock-out plants showed no significant differences in their F_v/F_m ratio. After AA treatment, the F_v/F_m ratio decreased in both genotypes but to a larger extent in *aox1a* mutants than in WT (Fig. 2A). These results suggest the importance of the AOX pathway in maintaining PSII efficiency at their maximum levels. After measurement of the F_v/F_m ratio, the AL was switched off (40 s) to allow the reaction centres of PSII to attain their oxidized state. Subsequently, various parameters related to chlorophyll fluorescence and P700 were recorded with every SP given up to 260 s at regular intervals of 20 s. In the absence of AA, a similar pattern of Y(II), ETR(II), q*P*, NPQ, Y(I), $P700_{red}$, Y(ND) and Y(NA) was observed for WT and *aox1a* plants (Figs 2B–E and 3). However, after AA treatment Y(II), ETR(II) and q*P* decreased significantly in *aox1a* compared with WT (Fig. 2B–D). By contrast, NPQ, an indicator of thermal dissipation, was increased in WT but remained unchanged in *aox1a* mutants (Fig. 2E). Similarly, Y(I) and the reduction state of P700 decreased drastically in *aox1a* compared with WT upon AA treatment (Fig. 3A, B). Y(ND) increased in both genotypes but to a larger extent in *aox1a* mutants. However, such an increase in Y(NA) was not observed in both WT and *aox1a* plants, irrespective of AA treatment (Fig. 3C, D). These results indicate that AOX1A plays a crucial role in maintaining the electron flow between PSII and PSI, and consequently ΔpH and thereby NPQ to dissipate excess energy in the form of heat.

Effect of AOX1A deficiency on cellular redox couples in the presence of AA

The role of the AOX pathway in regulating cellular redox homeostasis to optimize photosynthesis during oxidative stress was determined by monitoring changes in total cellular oxidized and reduced pools of redox couples related to NAD(H), NADP(H) and Asc (Figs 4 and 5).

In control samples, levels of $NAD(P)^+$ and NAD(P)H and the ratio of NAD(P)H to the total cellular pools of $NAD(P)^+$ plus NAD(P)H were similar in both WT and *aox1a* mutants (Fig. 4). Upon AA treatment, the increase in the ratio of NADH to the total cellular NAD^+ plus NADH pool was significant in *aox1a* mutants when compared with WT plants (Fig. 4C). In contrast, the redox ratio of NADPH to the total cellular $NADP^+$ plus NADPH pools increased significantly in both genotypes (Fig. 4F). In control samples, the cellular levels of Asc and its oxidized form DHA did not vary between WT and *aox1a*, while the redox ratios (Asc/DHA) were modulated marginally (Fig. 5). Upon AA treatment, Asc levels increased in WT but decreased in *aox1a* plants compared with their respective controls (Fig. 5A). By contrast, levels of DHA increased in both genotypes compared with their respective controls (Fig. 5B). Also, the Asc/DHA ratio decreased significantly in both genotypes in the presence, but not in the absence, of AA (Fig. 5C).

These results suggest that the deficiency of AOX1A did not alter the cellular redox state under control conditions. However,

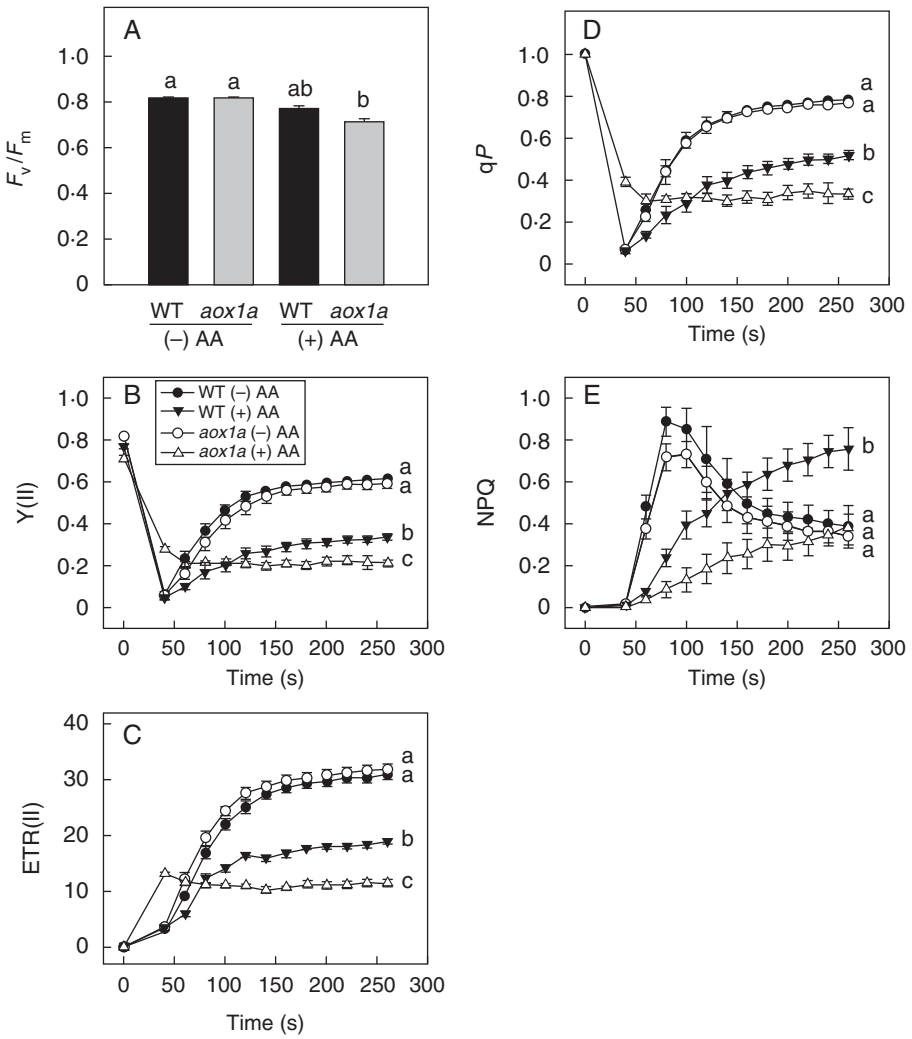

FIG. 2. Characteristics of chlorophyll fluorescence parameters in WT and *aox1a* from control (Tween-20) and treated (20 μM AA in Tween-20) leaf discs pre-illuminated (6 h) at a PPFD of 50 μmol m^{-2} s^{-1} at 25 °C: (A) maximum quantum yield of PSII (F_v/F_m), (B) relative quantum yield of PSII [Y(II)], (C) electron transport rate of photosystem II (ETRII), (D) photochemical quenching (q*P*), (E) non-photochemical quenching (NPQ). Other details for measurement of chlorophyll fluorescence parameters were as described in Materials and methods. Different lower-case letters indicate statistically significant differences ($P < 0{\cdot}05$).

upon restriction of the COX pathway, the cellular redox homeostasis was disturbed in both WT and *aox1a* genotypes. The imbalance in the cellular redox state was more prominent in *aox1a* than WT, indicating the important role of AOX1A in regulating cellular redox homeostasis and thereby photosynthetic performance.

Effect of AOX1A deficiency on intracellular ROS accumulation and membrane damage in the presence of AA

The role of AOX1A in alleviating cellular ROS and minimizing membrane damage as well as the optimization of photosynthetic performance of leaves during oxidative stress was evaluated by monitoring changes in cellular ROS levels as DCF fluorescence as well as H_2O_2 and MDA content (Figs 6 and 7). Furthermore, changes in chloroplastic ROS were differentiated from other cellular ROS by monitoring the pseudo orange/yellow colour formed due to superimposition of chlorophyll autofluorescence and DCF fluorescence. In control leaf discs, DCF fluorescence and orange/yellow fluorescence was marginally higher in *aox1a* knock-out mutants compared with WT (Fig. 6A). In contrast, after AA treatment, DCF as well as orange/yellow fluorescence increased significantly in *aox1a* mutants (Fig. 6B). In addition, both genotypes showed an increase in H_2O_2 levels and MDA content in the presence of AA (Fig. 7). The increase in H_2O_2 was more pronounced in *aox1a* than in WT compared with their respective controls (Fig. 7A). These results suggest that the deficiency of AOX1A caused an accumulation of total cellular as well as chloroplastic ROS.

Effect of AOX1A deficiency on gene expression of antioxidants, the malate–OAA shuttle and respiratory enzymes in the presence of AA

The role of AOX1A in regulating the malate–OAA shuttle and the antioxidative system during oxidative stress was

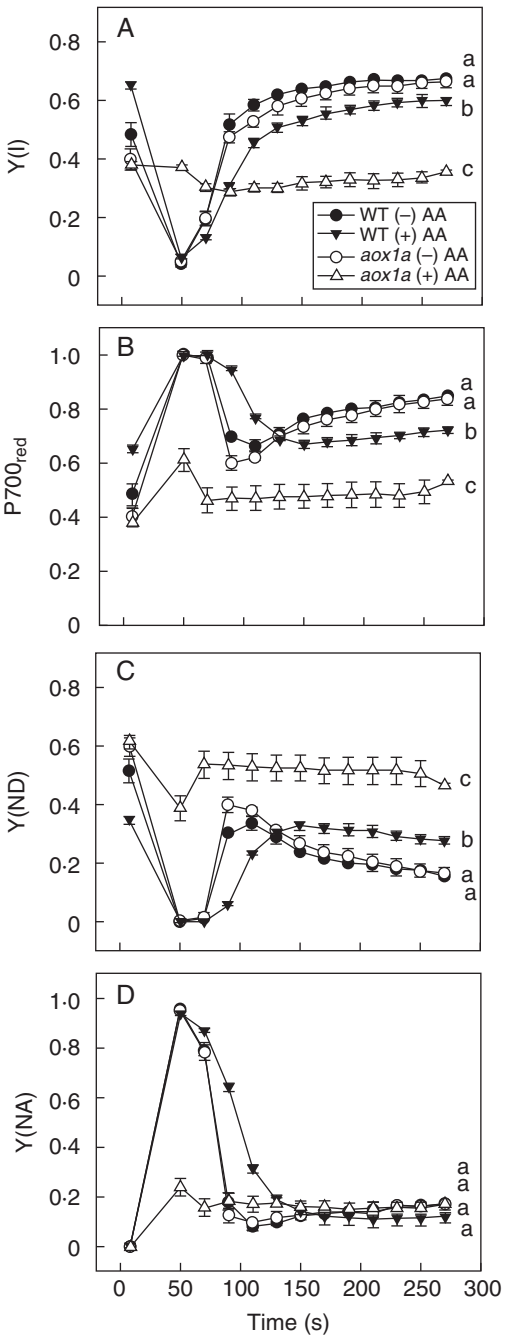

FIG. 3. Characteristics of P700 parameters in WT and *aox1a* from control (Tween-20) and treated (20 μM AA in Tween-20) leaf discs pre-illuminated (6 h) at a PPFD of 50 μmol m^{-2} s^{-1} at 25 °C: (A) quantum yield of PSI [Y(I)], (B) reduced P700 ($P700_{red}$), (C) limitation at the acceptor side of PSI [Y(NA)], (D) limitation at the donor side of PSI [Y(ND)]. Other details for measurement of P700 parameters were as described in Materials and methods. Different lowercase letters indicate statistically significant differences ($P < 0.05$).

monitored by evaluating changes in transcript levels of genes related to (1) respiratory metabolism: *PFK4* – phosphofructokinase, *AOX1A* – alternative oxidase and *COX15* – cytochrome oxidase; (2) malate–OAA shuttle: *chlMDH* – NADP-dependent chloroplastic malate dehydrogenase, *MMDH1* – NAD-dependent mitochondrial malate dehydrogenase and *ICDH* NADP-dependent chloroplastic/peroxisomal isocitrate dehydrogenase; and (iii) antioxidative enzymes: *CSD1* – cytosolic superoxide dismutase, *CAT1* – peroxisomal/chloroplastic catalase and *sAPX* – stromal ascorbate peroxidase (Fig. 8). The expression of *AOX1A* was notably increased in WT (18-fold) in the presence of AA, whereas no transcript could be detected in *aox1a* plants, as expected for this knock-out mutant (Fig. 8A). In the absence of AA, the expression of all genes examined in *aox1a* knock-out mutants was generally similar to WT except sAPX, which is increased in *aox1a* compared with WT (Fig. 8). Upon AA treatment, the expression of the glycolytic enzyme *PFK4* decreased in both genotypes compared with controls without AA (Fig. 8A). In contrast, the expression of *COX15* increased in WT, while it remained unchanged in *aox1a* (Fig. 8A). Similar to *PFK4*, in the presence of AA, the expression of *chlMDH*, *MMDH1* and *ICDH* genes related to the malate–OAA shuttle decreased in both genotypes (Fig. 8B). However, the decrease in the expression of *MMDH1* and *ICDH* was more pronounced in *aox1a* than in WT. By contrast, in the presence of AA, expression of the antioxidative genes *CSD1*, *CAT1* and *sAPX* increased in WT. These genes showed differential expression in *aox1a*. Transcript levels of *CSD1* increased, while *sAPX* decreased in leaf discs treated with AA, whereas *CAT1* expression was unchanged (Fig. 8C). These results suggest that during COX pathway inhibition, the deficiency of AOX1A not only perturbs respiratory metabolism but also modulates the antioxidative system in order to balance ROS generation and detoxification.

Overall, the results of the present study revealed the impact of deficiency of AOX1A on mitochondrial respiration and chloroplastic photosynthesis when electron transport through the COX pathway is restricted, which is schematically represented in Fig. 9.

DISCUSSION

The dependence of chloroplastic photosynthesis on mitochondrial respiration is well documented (Raghavendra *et al*., 1994; Krömer, 1995; Padmasree *et al*., 2002; Fernie *et al*., 2004; Raghavendra and Padmasree, 2003; Noguchi and Yoshida, 2008; Vanlerberghe, 2013). Different components of mitochondrial respiration, including the Krebs cycle, electron transport, oxidative phosphorylation and UCP, were found to be important to sustain photosynthetic performance during normal growth or under various biotic/abiotic stress conditions (Krömer *et al*., 1993; Padmasree and Raghavendra, 1999*a*; Sweetlove *et al*., 2006; Dinakar *et al*., 2010*b*; Yoshida *et al*., 2011*a*; Araújo *et al*., 2012, 2014; Gandin *et al*., 2014*a*). The relative importance and contribution of the COX and AOX pathways in benefiting different components of photosynthesis such as carbon assimilation, photochemical reactions, photosynthetic induction and light activation of Calvin cycle enzymes was revealed in several model plants using specific metabolic inhibitors as well as transgenic/reverse genetic approaches (Padmasree and Raghavendra, 1999*a*, *b*, 2001; Yoshida *et al*., 2006; Dinakar *et al*., 2010*a*; Zhang *et al*., 2011; Zhang *et al*., 2014). Furthermore, the significant role of the AOX1A isoform over AOX1D in coordinating the COX pathway to optimize photosynthesis was established in a previous

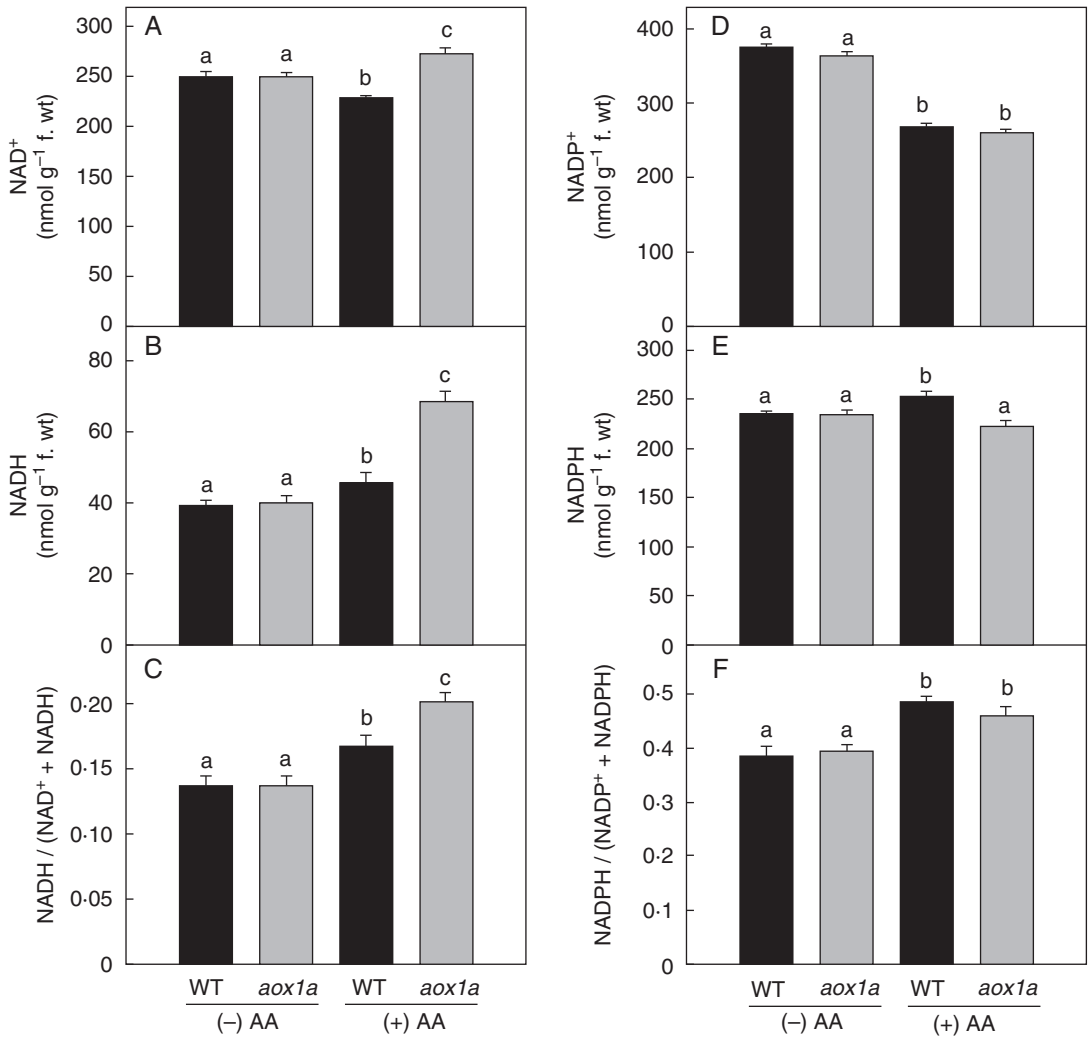

FIG. 4. Changes in total cellular oxidized and reduced pools of redox couples related to NAD(H) and NADP(H) and their redox ratio in WT and *aox1a* from control (Tween-20) and treated (20 μM AA in Tween-20) leaf discs pre-illuminated (6 h) at a PPFD of 50 μmol m^{-2} s^{-1} at 25 °C: (A) NAD^+, (B) NADH, (C) NADH/(NAD^++NADH) ratio, (D) $NADP^+$, (E) NADPH and (F) NADPH/($NADP^+$+NADPH) ratio. Pyridine nucleotide contents were calculated with their corresponding standards. Other details for measurement of NAD(P) and NAD(P)H were as described in Materials and methods. Different lower-case letters indicate statistically significant differences ($P < 0{\cdot}05$).

study (Strodtkötter *et al*., 2009). In the present study, we investigated the physiological role of AOX1A in regulating cellular redox homeostasis and ROS generation to benefit different components of photosynthesis when electron transport through the COX pathway of the mETC is restricted at complex III.

Essentiality of AOX1A for optimal photosynthetic performance and chloroplastic heat dissipation

The use of *aox1a* mutants along with AA treatment allowed us to analyse the state of COX pathway restriction in the background of an impaired AOX pathway, whereas the treatment of WT with AA resulted only in COX pathway restriction. Restriction of the electron transport through complex III was ascertained by monitoring the decrease in rates of respiratory O_2 uptake with increasing concentrations of AA (Fig. 1A). Interference of the mETC through complex III caused a drastic reduction in both photosynthetic carbon assimilation and photochemical reactions in *aox1a* mutants compared with WT (Figs 1B, 2 and 3). Strodtkötter *et al*. (2009) showed that induction of AOX1D compromised the function of AOX1A in T-DNA insertion mutants of *aox1a*. However, in spite of the expression of AOX1D, *aox1a* mutants could neither maintain respiration nor their photosynthetic performance compared with WT plants when electron transport through the COX pathway is inhibited.

AA is well known to bind to the Q_i site of the cyt_{bc1} complex in mETC (Xia *et al*., 1997). However, its effect on cyclic electron flow around PSI (CEF-PSI) was also reported (Endo *et al*., 1998; Munekage *et al*., 2004). Such interference of AA on CEF-PSI might be small or negligible in the present study for the following reasons: (1) the concentration of AA required to inhibit CEF-PSI is 10–100 times higher than that required to in

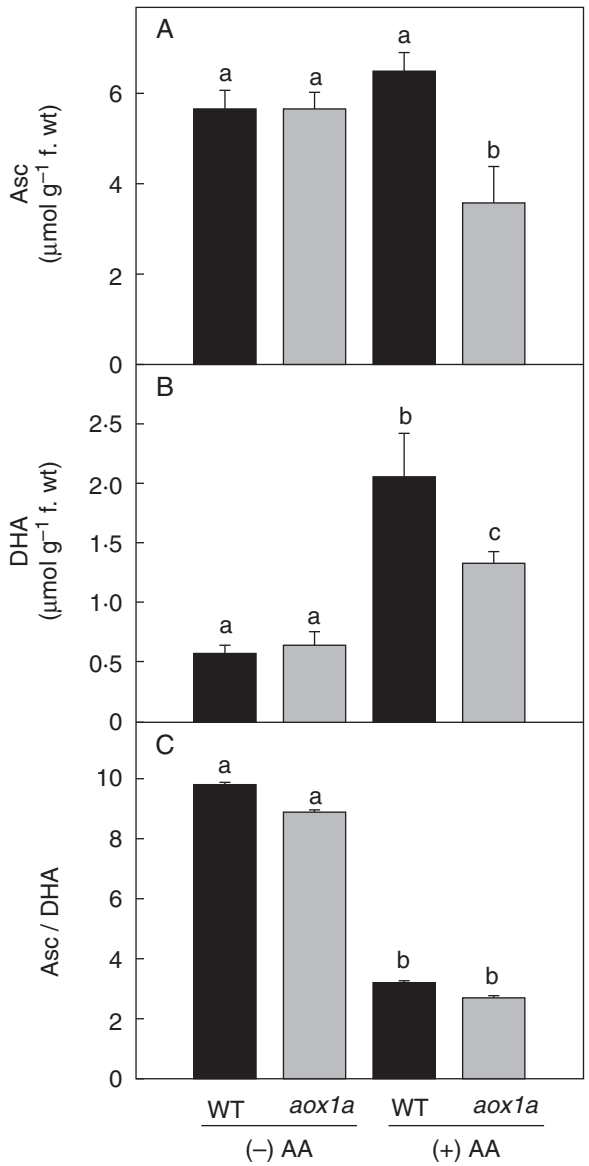

FIG. 5. Changes in total cellular oxidized and reduced pools of Asc redox couple in WT and *aox1a* from control (Tween-20) and treated (20 µM AA in Tween-20) leaf discs pre-illuminated (6 h) at a PPFD of 50 µmol m^{-2} s^{-1} at 25 °C; (A) Asc, (B) DHA and (C) Asc/DHA ratio. Other details for measurement of Asc were as described in Materials and methods. Different lower-case letters indicate statistically significant differences ($P < 0{\cdot}05$).

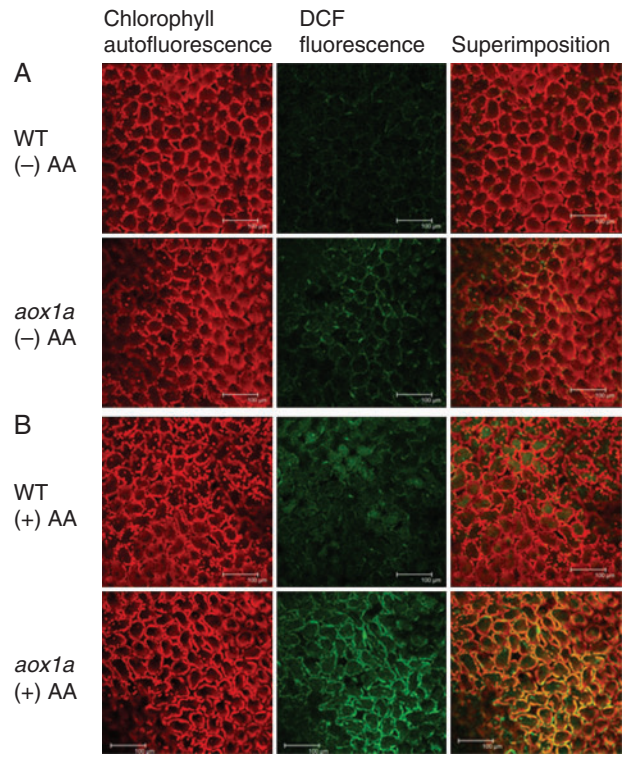

FIG. 6. Measurement of ROS formation in WT and *aox1a* from (A) control (Tween-20) and (B) treated (20 µM AA in Tween-20) leaf discs pre-illuminated (6 h) at a PPFD of 50 µmol m^{-2} s^{-1} at 25 °C using confocal laser scanning microscopy. Chlorophyll autofluorescence is shown in red, DCF fluorescence, which represents cellular ROS, is shown in green and superimposed images representing chloroplastic ROS in pseudo orange/yellow. All scale bars = 100 µm.

hibit the COX pathway (Taira *et al.*, 2013); (2) the effects of AA on respiration and photosynthesis were found to be biphasic in the present study. For instance, the treatment of WT leaf discs with ≤20 µM AA caused only <18 % decrease in rates of both respiration and photosynthesis, while treatment with ≥20 µM AA caused a drastic decrease of ≤70 % in their rates (Fig. 1); (3) the total cellular levels of ATP as well as the ATP/ADP ratio were higher in *aox1a* plants (with and without AA treatment) compared with WT (without AA) in both protoplasts and leaf discs (Supplementary Data Fig. S1; Strodtkötter *et al.*, 2009); and (4) the effects of AA on most of the parameters examined in the present study were always less pronounced in WT than in *aox1a* plants (Figs 1–8). Unlike the protoplasts or cyanobacteria (Yeremenko *et al.*, 2005) where AA is easily permeable through plasma/cell membranes, leaf discs are less permeable to AA. Hence, effective concentrations of AA that ultimately reach chloroplasts at the cellular level are expected to be much less than 20 µM. Moreover, the effect of 20 µM AA observed in respiratory and photosynthetic rates of *aox1a* leaf discs in the present study corroborated well with the effects examined on mesophyll protoplasts of *aox1a* knock-out mutants (Fig. 1; Strodtkötter *et al.*, 2009). Thus, AA was used at 20 µM in all further studies to exemplify the physiological role of AOX1A in optimizing photosynthesis.

Linear electron flow and CEF-PSI are coupled to proton pumping across the thylakoid membrane, resulting in acidification of the thylakoid lumen, thereby generating a proton gradient (ΔpH). This ΔpH is utilized for ATP synthesis and NPQ induction (Shikanai, 2007, 2014). The impact of the proton gradient on NPQ induction was evident through an Arabidopsis *pgr5* (proton gradient regulation) mutant (defective in CEF), which showed a lower NPQ at high irradiance (Yoshida *et al.*, 2011*b*). Although the role of AOX1A in modulating NPQ was not shown in their study, several other studies have demonstrated that the lack of AOX caused a significant decrease in quantum yield of PSII, ETR and NPQ under HL conditions (Zhang *et al.*, 2010; Zhang *et al.*, 2012; Vishwakarma *et al.*, 2014). Furthermore, *aox1a pgr5* double mutants showed a significant decrease in CEF-PSI compared with *pgr5*, indicating the synergetic function of AOX1A and CEF-PSI (Yoshida

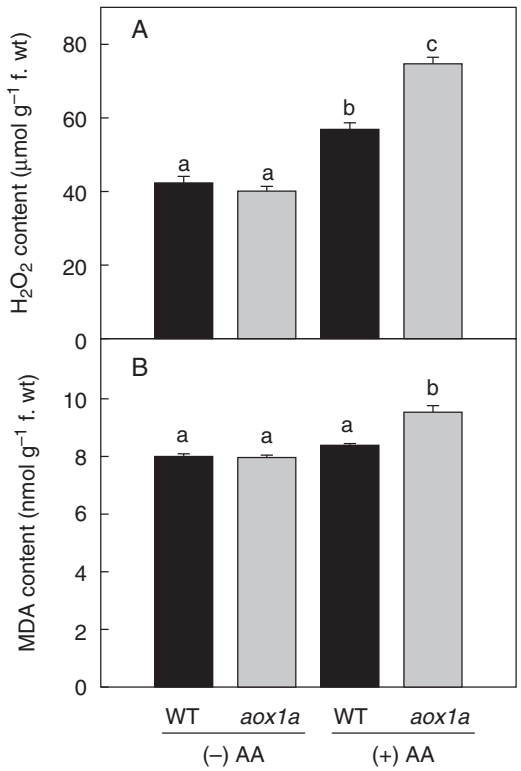

FIG. 7. Quantification of H_2O_2 formation (A) and lipid peroxidation as MDA content (B) in WT and *aox1a* from control (Tween-20) and treated (20 μM AA in Tween-20) leaf discs pre-illuminated (6 h) at a PPFD of 50 μmol m^{-2} s^{-1} at 25 °C. Further details were as described in Materials and methods. Different lower-case letters indicate statistically significant differences ($P < 0{\cdot}05$).

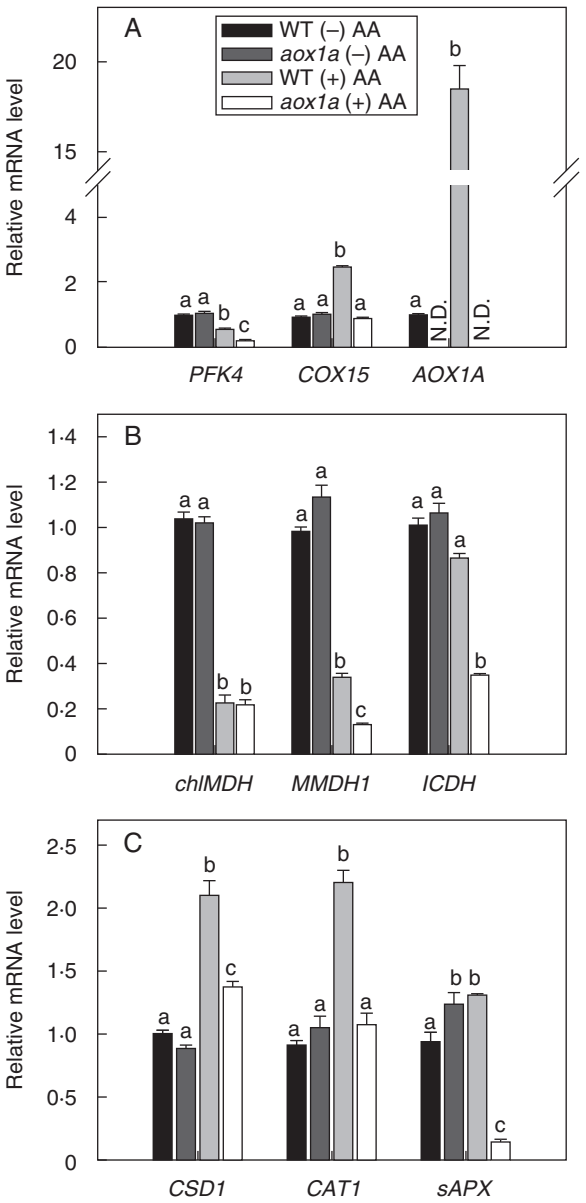

FIG. 8. Gene expression profiles in WT and *aox1a* from control (Tween-20) and treated (20 μM AA in Tween-20) leaf discs pre-illuminated (6 h) at a PPFD of 50 μmol m^{-2} s^{-1} at 25 °C: (A) respiratory enzymes (*PFK4*, *COX15* and *AOX1A*), (B) malate–OAA shuttle enzymes (*MMDH1*, *chlMDH* and *ICDH*) and (C) antioxidative enzymes (*CSD1*, *CAT1* and *sAPX*). N.D. denotes expression of gene was not detected (A). Transcript abundance was quantified by the $\Delta\Delta C_T$ method using *UBQ5* as a reference gene. Further details were as described in Materials and methods. Different lower-case letters indicate statistically significant differences ($P < 0{\cdot}05$).

et al., 2011*b*). In Arabidopsis, the targeting of AOX1A and AOX2 into chloroplasts using its own transit peptide resulted in induction of NPQ and also suggested that these isoforms have the ability to substitute the function of plastid terminal oxidase (PTOX, an analogue of AOX), which mediates the electron flow from PQ to O_2 and thus prevent the over reduction of PQ during excess light (McDonald *et al.*, 2011; Fu *et al.*, 2012). In the present study, although PTOX activity was not measured directly, a significant decrease in ETR(II) and NPQ in *aox1a* mutants compared with WT plants suggests that PTOX could not compensate for the lack of AOX1A. Furthermore, an increase in Y(ND) in *aox1a* mutants indicates the down-regulation of PSII due to donor-side limitation of PSI, as evident by a decrease in ETR(II), Y(II) and q*P* (Figs 2B–D and 3C). Taken together, these results demonstrate that AOX1A plays a crucial role in maintaining the balanced electron flow between PSI and PSII, and thereby ΔpH and NPQ induction, which protect photosynthesis from photoinhibition when electron flow through the COX pathway is restricted.

AOX1A maintains the redox balance between photochemical reactions and the Calvin cycle by regulating the malate valve to dissipate excess chloroplastic reducing equivalents

During active photosynthesis, photochemical reactions generate reducing equivalents at much higher magnitudes than their demands in the Calvin cycle. Under such conditions, excess reducing equivalents are transported to peroxisomes or mitochondria via the cytosol through the malate valve, which allows the exchange of malate for OAA across the chloroplast membrane via specific transporters (Noguchi and Yoshida, 2008; Weber and Linka, 2011). The mitochondrial electron transport chain oxidizes these reducing equivalents by external/internal NAD(P)H dehydrogenases and AOX (Rasmusson *et al.*, 2004; Noguchi and Yoshida, 2008). The activity of the enzymes

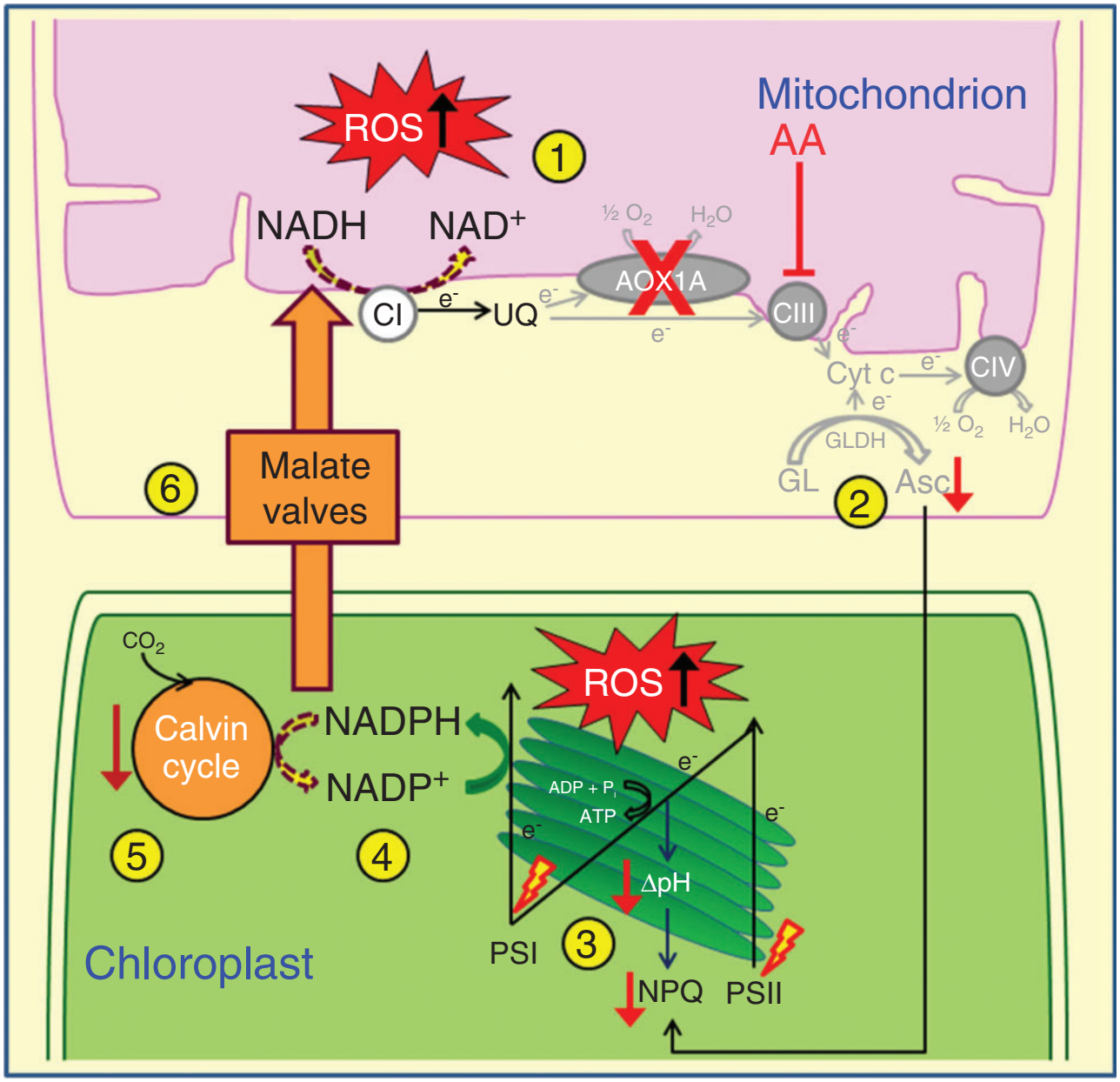

FIG. 9. A simple scheme illustrating the impact of AOX1A deficiency on mitochondrial respiration and chloroplastic photosynthesis, when electron transport through the COX pathway is restricted at complex III using AA in leaf discs of Arabidopsis under growth light conditions: (1) over-reduction of mETC and ROS accumulation due to restricted COX and AOX pathways; (2) decrease in Asc biosynthesis; (3) low thylakoid energization; (4) acceptor limitation at PSI; (5) decrease in photosynthetic carbon assimilation; (6) lack of electron sink in mitochondria leads to impairment of photosynthesis. The broken lined arrows indicate a reduction in utilization of reducing equivalents. AA, antimycin A; AOX1A, alternative oxidase 1a; Asc, ascorbate; CI, complex I; CIII, complex III; CIV, complex IV; mETC, mitochondrial electron transport chain; GL, L-galactono-1,4-lactone; GLDH, L-galactono-1,4-lactone dehydrogenase; NPQ, non-photochemical quenching; PSI, photosystem I; PSII, photosystem II; ROS, reactive oxygen species; UQ, ubiquinone.

NADP-MDH, NAD-MDH, citrate synthase (CS), NADP-ICDH and NAD-ME, which are known to actively coordinate the malate–OAA shuttle, were significantly increased in *aox1a* knock-out plants compared with WT under HL conditions in order to prevent an over-reduction of chloroplastic electron transport carriers (Zhang *et al.*, 2010; Xu *et al.*, 2011). Furthermore, the *aox1a* mutants exhibited an increase in NAD(P)H levels and redox ratios of their corresponding redox couples under HL conditions when compared with WT plants. This indicates the significance of AOX1A in oxidizing excess reducing equivalents (Vishwakarma *et al.*, 2014). Similarly, in the present study *aox1a* plants showed an excess NADH level compared with WT when the COX pathway is restricted (Fig. 4B). By contrast, NADPH levels did not further increase in *aox1a* mutants compared with WT plants as expected (Fig. 4E). This is because, as *aox1a* is more prone to oxidative damage caused by AA compared with WT, which is evident by the increase in H_2O_2 and MDA content (Fig. 7), it might exhibit

metabolic adjustments to oxidize/utilize excess NADPH in the following reactions: (1) generation of O_2^- by NADPH oxidase (Sagi and Fluhr, 2006; Andronis *et al*., 2014); (2) photorespiration, as evident by an increase in the glycine decarboxylase P-protein in *aox1a* plants after treatment with AA (Strodtkötter *et al*., 2009; Voss *et al*., 2013); and (3) ascorbate–glutathione cycle or glutathione cycle to scavenge H_2O_2 by ascorbate peroxidase or glutathione peroxidase (Foyer and Noctor, 2011; Gill *et al*., 2013). However, a pronounced increase in the ratio of the NADH redox couple as well as the decrease in transcript levels of *MMDH1* and *ICDH* in *aox1a* mutants implicated the importance of AOX1A in relieving excess reductive pressure on chloroplastic redox carriers by regulating the malate valve particularly when the COX pathway is compromised (Figs 4C and 8B).

Significance of AOX1A in regulating cellular ROS and antioxidative system

The AOX pathway plays a significant role in the dissipation of chloroplastic reducing equivalents through the malate valve and prevents the over-reduction of mETC carriers. Such a role was hypothesized earlier by using salicylhydroxamic acid (SHAM), an inhibitor of the AOX pathway, and was further confirmed in the present study by using *aox1a* mutants (Padmasree and Raghavendra, 1999*c*; Yoshida *et al*., 2006; Figs 4 and 8B). Therefore, the likelihood of electron leakage from mETC is expected to be higher in AA-treated *aox1a* mutants (Møller, 2001; Strodtkötter *et al*., 2009; Yoshida *et al*., 2011*a*). When single electrons react with molecular oxygen, ROS (OH^-, O_2^- and H_2O_2) are generated which can influence the expression of the genes related to antioxidative strategies by modifying transcription factors through retrograde regulatory mechanisms (Apel and Hirt, 2004; Choudhury *et al*., 2013; Li *et al*., 2013). These include biosynthesis of carotenoids and flavonoids, the xanthophyll cycle, water–water cycle, NPQ, photorespiration and ROS scavenging enzymes (Niyogi, 2000; Murchie and Niyogi, 2011). If cellular ROS generation exceeds the scavenging capacity of the above mentioned defence strategies, it leads to oxidative stress and ROS can damage various cellular structures including DNA, proteins, lipids or cell walls (Foyer and Noctor, 2005; Gill and Tuteja, 2010; del Río, 2015). During salt stress, the activity and transcript levels of antioxidative enzymes were shown to be significantly increased to scavenge excess ROS (Wang *et al*, 2010). In agreement with this, in the present study, AA treatment induced the expression of antioxidative genes in WT plants, and hence ROS accumulation was less, which is not the case in *aox1a* mutants (Figs 6B, 7A and 8C). In *aox1a* mutants, AA treatment resulted in an accumulation of total cellular ROS including chloroplastic ROS, as indicated by localization of DCF fluorescence in those areas which contain high chlorophyll autofluorescence (Fig. 6B). Furthermore, the increase in membrane damage under these conditions was evident from the increase in MDA content (Fig. 7B). The expression of antioxidative genes was much lower in AA-treated *aox1a* mutants which could be due to partial impairment of antioxidative systems. This may explain AOX1A signalling in the induction of antioxidative enzymes and/or synergistic expression of *AOX1A* and antioxidative genes (Fig. 8A).

The cellular redox state also plays an important role in mediating the signalling linked to developmental processes or environmental changes (Foyer and Noctor, 2005; Suzuki *et al*., 2012). NAD^+, $NADP^+$, glutathione and Asc, the key players of the ascorbate–glutathione cycle, interact strongly with ROS to maintain cellular redox homeostasis (Noctor, 2006). Among ROS, H_2O_2 is more stable than O_2^- and $^1O_2$. Asc, the most abundant antioxidant in plant cells, is oxidized by H_2O_2 to monodehydroascorbate (MDHA) in the presence of ascorbate peroxidase (APX) and is efficiently recycled back by the action of monodehydroascorbate reductase (MDHAR) or dehydroascorbate reductase (DHAR) (Smirnoff, 2000). Thus, Asc plays an important role in the detoxification of ROS under various stress conditions. In the present study, the pronounced decrease in Asc and *sAPX* levels along with reduction in respiratory O_2 uptake or photosynthetic O_2 evolution in *aox1a* mutants upon treatment with AA as opposed to WT plants indicate the relative importance of AOX1A over the COX pathway in regulating the antioxidative system to optimize photosynthesis (Figs 1, 5A and 8C; Yabuta *et al*., 2007; Dinakar *et al*., 2010*a*). Furthermore, the increase in Asc levels parallels an increase in *COX15* in WT but not in *aox1a* plants, suggesting a role of the AOX pathway in regulating Asc biosynthesis (Figs 5A and 8A; Bartoli *et al*., 2000). Moreover, Asc is a cofactor of violaxanthin de-epoxidase, which activates the zeaxanthin-dependent qE (energy-dependent quenching) and thus induces NPQ (Tóth *et al*., 2013). In the present study, after restriction of complex III, a decrease in NPQ in *aox1a* mutants could also be due to low Asc levels (Figs 2E and 5A). The importance of ROS, antioxidative metabolites and antioxidative enzymes in mediating beneficial interactions between mitochondrial respiration and chloroplastic photosynthesis was shown in *Pisum sativum* (Dinakar *et al*., 2010*a*).

Thus, the present study suggests the physiological importance of AOX1A in performing mitochondrial and extramitochondrial functions to optimize chloroplastic photosynthesis when electron transport through the COX pathway is restricted (Fig. 9). In mitochondria, AOX1A plays a role: (1) in the maintenance of mETC redox homeostasis; (2) preventing accumulation of reducing equivalents and thereby ROS generation; and (3) regulation of Asc biosynthesis. On the other hand, AOX1A performs the following functions outside the mitochondria: (1) sustaining photosynthetic carbon assimilation; (2) induction of NPQ; (3) operation of the malate–OAA shuttle to dissipate excess chloroplastic reducing equivalents and recycle redox carriers; (4) maintenance of redox homeostasis by preventing the over-reduction of chloroplastic ETC carriers and ROS generation; and (5) coordinate with antioxidative systems to maintain cellular ROS at optimal levels.

SUPPLEMENTARY DATA

Supplementary data are available online at www.aob.oxfordjournals.org and consist of the following. Table S1: Details of primers used for real-time PCR. Figure S1: Measurement of total content of ATP, ADP and their corresponding ratio in WT and *aox1a* from control and treated leaf discs.

ACKNOWLEDGEMENTS

This work was supported by grants to K.P. (PI) and S.D.T. (Co-PI) from the Department of Biotechnology, New Delhi

(No. BT/PR10272/GBD/27/85/2007), while the concept was initiated during the stays (2005–2006 and 2007) of K.P. as an AvH Research Fellow in the laboratory of R.S. J.S. thanks the University of Osnabrück for Research Fund, and A.V. is grateful to CSIR for a Senior Research Fellowship. We thank Prof. A. S. Raghavendra from the University of Hyderabad for critical suggestions while implementing the experiments. We thank Ms Nalini and Mrs Leena for their technical assistance with confocal microscopy and real-time PCR, respectively. The departmental/school facilities of the University of Hyderabad were supported by grants from DST-FIST, UGC-SAP-CAS, DBT-CREBB, DST-PURSE, UPE and UGC-DRS, all from New Delhi, India. No conflict of interest is declared.

LITERATURE CITED

Andronis EA, Moschou PN, Toumi I, Roubelakis-Angelakis KA. 2014. Peroxisomal polyamine oxidase and NADPH-oxidase cross-talk for ROS homeostasis which affects respiration rate in *Arabidopsis thaliana*. *Frontiers in Plant Science* **5**: 132

Apel K, Hirt H. 2004. Reactive oxygen species: metabolism, oxidative stress, and signal transduction. *Annual Review of Plant Biology* **55**: 373–99.

Araújo WL, Nunes-Nesi A, Nikoloski Z, Sweetlove LJ, Fernie AR. 2012. Metabolic control and regulation of the tricarboxylic acid cycle in photosynthetic and heterotrophic plant tissues. *Plant Cell Environment* **35**: 1–21.

Araújo WL, Nunes-Nesi A, Fernie AR. 2014. On the role of plant mitochondrial metabolism and its impact on photosynthesis in both optimal and sub-optimal growth conditions. *Photosynthesis Research* **119**: 141–156.

Arnholdt-Schmitt B, Costa JH, de Melo DF. 2006. AOX–a functional marker for efficient cell reprogramming under stress? *Trends in Plant Science* **11**: 281–287.

Bartoli CG, Pastori GM, Foyer CH. 2000. Ascorbate biosynthesis in mitochondria is linked to the electron transport chain between complexes III and IV. *Plant Physiology* **123**: 335–343.

Bartoli CG, Yu J, Gómez F, Fernández L, McIntosh L, Foyer CH. 2006. Inter-relationships between light and respiration in the control of ascorbic acid synthesis and accumulation in *Arabidopsis thaliana* leaves. *Journal of Experimental Botany* **57**: 1621–1631.

Choudhury S, Panda P, Sahoo L, Panda SK. 2013. Reactive oxygen species signaling in plants under abiotic stress. *Plant Signaling and Behavior* **8**: e23681.

Clifton R, Lister R, Parker KL, *et al.* 2005. Stress-induced co-expression of alternative respiratory chain components in *Arabidopsis thaliana*. *Plant Molecular Biology* **58**: 193–212.

Clifton R, Millar AH, Whelan J. 2006. Alternative oxidases in Arabidopsis: a comparative analysis of differential expression in the gene family provides new insights into function of non-phosphorylating bypasses. *Biochimica et Biophysica Acta* **1757**: 730–741.

Considine MJ, Holtzapffel RC, Day DA, Whelan J, Millar AH. 2002. Molecular distinction between alternative oxidase from monocots and dicots. *Plant Physiology* **129**: 949–953.

Cvetkovska M, Vanlerberghe GC. 2012. Coordination of a mitochondrial superoxide burst during the hypersensitive response to bacterial pathogen in *Nicotiana tabacum*. *Plant Cell Environment* **35**: 1121–1136.

Cvetkovska M, Dahal K, Alber NA, Jin C, Cheung M, Vanlerberghe GC. 2014. Knockdown of mitochondrial alternative oxidase induces the 'stress state' of signaling molecule pools in *Nicotiana tabacum*, with implications for stomatal function. *New Phytologist* **203**: 449–461.

del Río LA. 2015. ROS and RNS in plant physiology: an overview. *Journal of Experimental Botany* **66**: 2827–2837.

Dinakar C, Abhaypratap V, Yearla SR, Raghavendra AS, Padmasree K. 2010a. Importance of ROS and antioxidant system during the beneficial interactions of mitochondrial metabolism with photosynthetic carbon assimilation. *Planta* **231**: 461–474.

Dinakar C, Raghavendra AS, Padmasree K. 2010b. Importance of AOX pathway in optimizing photosynthesis under high light stress: role of pyruvate and malate in activating AOX. *Physiologia Plantarum* **139**: 13–26.

Endo T, Shikanai T, Sato F, Asada K. 1998. NAD(P)H dehydrogenase-dependent, antimycin A-sensitive electron donation to plastoquinone in tobacco chloroplasts. *Plant Cell Physiology* **39**: 1226–1231.

Feng H, Li H, Li X, *et al.* 2007. The flexible interrelation between AOX respiratory pathway and photosynthesis in rice leaves. *Plant Physiology and Biochemistry* **45**: 228–235.

Fernie AR, Carrari F, Sweetlove LJ. 2004. Respiratory metabolism: glycolysis, the TCA cycle and mitochondrial electron transport. *Current Opinion in Plant Biology* **7**: 254–261.

Foyer CH, Noctor G. 2005. Redox homeostasis and antioxidant signaling: a metabolic interface between stress perception and physiological responses. *Plant Cell* **17**: 1866–75.

Foyer CH, Noctor G. 2011. Ascorbate and glutathione: the heart of the redox hub. *Plant Physiology* **155**: 2–18.

Foyer C, Rowell J, Walker D. 1983. Measurement of the ascorbate content of spinach leaf protoplasts and chloroplasts during illumination. *Planta* **157**: 239–244.

Fu A, Liu H, Yu F, Kambakam S, Luan S, Rodermel S. 2012. Alternative oxidases (AOX1a and AOX2) can functionally substitute for plastid terminal oxidase in Arabidopsis chloroplasts. *Plant Cell* **24**: 1579–1595.

Gandin A, Duffes C, Day DA, Cousins AB. 2012. The absence of alternative oxidase AOX1A results in altered response of photosynthetic carbon assimilation to increasing CO_2 in *Arabidopsis thaliana*. *Plant Cell Physiology* **53**: 1627–1637.

Gandin A, Denysyuk M, Cousins AB. 2014a. Disruption of the mitochondrial alternative oxidase (AOX) and uncoupling protein (UCP) alters rates of foliar nitrate and carbon assimilation in *Arabidopsis thaliana*. *Journal of Experimental Botany* **65**: 3133–3142.

Gandin A, Koteyeva NK, Voznesenskaya EV, Edwards GE, Cousins AB. 2014b. The acclimation of photosynthesis and respiration to temperature in the C3-C4 intermediate *Salsola divaricata*: induction of high respiratory CO_2 release under low temperature. *Plant Cell Environment* **37**: 2601–2612.

Garmash EV, Grabelnych OI, Velegzhaninov IO, *et al.* 2015. Light regulation of mitochondrial alternative oxidase pathway during greening of etiolated wheat seedlings. *Journal of Plant Physiology* **174**: 75–84.

Gill SS, Tuteja N. 2010. Reactive oxygen species and antioxidant machinery in abiotic stress tolerance in crop plants. *Plant Physiology and Biochemistry* **48**: 909–930.

Gill SS, Anjum NA, Hasanuzzaman M, *et al.* 2013. Glutathione and glutathione reductase: a boon in disguise for plant abiotic stress defense operations. *Plant Physiology and Biochemistry* **70**: 204–212.

Giraud E, Ho LH, Clifton R, *et al.* 2008. The absence of ALTERNATIVE OXIDASE1a in Arabidopsis results in acute sensitivity to combined light and drought stress. *Plant Physiology* **147**: 595–610.

Gupta KJ, Igamberdiev AU, Mur LA. 2012. NO and ROS homeostasis in mitochondria: a central role for alternative oxidase. *New Phytologist* **195**: 1–3.

Hara S, Motohashi K, Arisaka F, *et al.* 2006. Thioredoxin-h1 reduces and reactivates the oxidized cytosolic malate dehydrogenase dimer in higher plants. *Journal of Biological Chemistry* **281**: 32065–32071.

Heath RL, Packer L. 1968. Photoperoxidation in isolated chloroplasts. I. Kinetics and stoichiometry of fatty acid peroxidation. *Archives of Biochemistry and Biophysics* **125**: 189–198.

Igamberdiev AU, Ratcliffe RG, Gupta KJ. 2014. Plant mitochondria: source and target for nitric oxide. *Mitochondrion* **19**: 329–333.

Klughammer C, Schreiber U. 2008. Complementary PS II quantum yields calculated from simple fluorescence parameters measured by PAM fluorometry and the Saturation Pulse method. *PAM Application Notes* **1**: 11–14.

Krömer S. 1995. Respiration during photosynthesis. *Annual Review of Plant Biology* **46**: 45–70.

Krömer S, Malmberg G, Gardeström P. 1993. Mitochondrial contribution to photosynthetic metabolism: a study with barley (*Hordeum vulgare* L.) leaf protoplasts at different light intensities and CO_2 concentrations. *Plant Physiology* **102**: 947–955.

Li CR, Liang DD, Li J, *et al.* 2013. Unravelling mitochondrial retrograde regulation in the abiotic stress induction of rice ALTERNATIVE OXIDASE 1 genes. *Plant Cell Environment* **36**: 775–788.

Livak KJ, Schmittgen TD. 2001. Analysis of relative gene expression data using real-time quantitative PCR and the $2^{\Delta\Delta CT}$ method. *Methods* **25**: 402–408.

McDonald AE, Ivanov AG, Bode R, Maxwell DP, Rodermel SR, Hüner NP. 2011. Flexibility in photosynthetic electron transport: the physiological role of plastoquinol terminal oxidase (PTOX). *Biochimica et Biophysica Acta - Bioenergetics* **1807**: 954–967.

Meeuse BJ. 1975. Thermogenic respiration in aroids. *Annual Review of Plant Physiology* **26**: 117–126.

Millenaar F, Lambers H. 2003. The alternative oxidase: in vivo regulation and function. *Plant Biology* **5**: 2–15.

Miller RE, Grant NM, Giles L, *et al.* 2011. In the heat of the night-alternative pathway respiration drives thermogenesis in *Philodendron bipinnatifidum*. *New Phytologist* **189**: 1013–1026.

Møller IM. 2001. Plant mitochondria and oxidative stress: electron transport, NADPH turnover, and metabolism of reactive oxygen species. *Annual Review of Plant Physiology and Plant Molecular Biology* **52**: 561–591.

Munekage Y, Hashimoto M, Miyake C, *et al.* 2004. Cyclic electron flow around photosystem I is essential for photosynthesis. *Nature* **429**: 579–582.

Murakami Y, Toriyama K. 2008. Enhanced high temperature tolerance in transgenic rice seedlings with elevated levels of alternative oxidase, OsAOX1a. *Plant Biotechnology* **25**: 361–364.

Murchie EH, Niyogi KK. 2011. Manipulation of photoprotection to improve plant photosynthesis. *Plant Physiology* **155**: 86–92.

Niyogi KK. 1999. Photoprotection revisited: genetic and molecular approaches. *Annual Review of Plant Biology* **50**: 333–359.

Niyogi KK. 2000. Safety valves for photosynthesis. *Current Opinion in Plant Biology* **3**: 455–460.

Noctor G. 2006. Metabolic signalling in defence and stress: the central roles of soluble redox couples. *Plant Cell Environment* **29**: 409–425.

Noguchi K, Terashima I. 2006. Responses of spinach leaf mitochondria to low N availability. *Plant Cell Environment* **29**: 710–719.

Noguchi K, Yoshida K. 2008. Interaction between photosynthesis and respiration in illuminated leaves. *Mitochondrion* **8**: 87–99.

Padmasree K, Raghavendra AS. 1999*a*. Importance of oxidative electron transport over oxidative phosphorylation in optimizing photosynthesis in mesophyll protoplasts of pea (*Pisum sativum* L.). *Physiologia Plantarum* **105**: 546–553.

Padmasree K, Raghavendra AS. 1999*b*. Response of photosynthetic carbon assimilation in mesophyll protoplasts to restriction on mitochondrial oxidative metabolism: metabolites related to the redox status and sucrose biosynthesis. *Photosynthesis Research* **62**: 231–239.

Padmasree K, Raghavendra AS. 1999*c*. Prolongation of photosynthetic induction as a consequence of interference with mitochondrial oxidative metabolism in mesophyll protoplasts of the pea (*Pisum sativum* L.). *Plant Science* **142**: 29–36.

Padmasree K, Raghavendra AS. 2001. Consequence of restricted mitochondrial oxidative metabolism on photosynthetic carbon assimilation in mesophyll protoplasts: decrease in light activation of four chloroplastic enzymes. *Physiologia Plantarum* **112**: 582–588.

Padmasree K, Padmavathi L, Raghavendra AS. 2002. Essentiality of mitochondrial oxidative metabolism for photosynthesis: optimization of carbon assimilation and protection against photoinhibition. *Critical Review of Biochemistry and Molecular Biology* **37**: 71–119.

Palmieri F, Rieder B, Ventrella A, *et al.* 2009. Molecular identification and functional characterization of *Arabidopsis thaliana* mitochondrial and chloroplastic NAD^+ carrier proteins. *Journal of Biological Chemistry* **284**: 31249–31259.

Queval G, Noctor G. 2007. A plate reader method for the measurement of NAD, NADP, glutathione, and ascorbate in tissue extracts: application to redox profiling during Arabidopsis rosette development. *Analytical Biochemistry* **363**: 58–69.

Raghavendra AS, Padmasree K. 2003. Beneficial interactions of mitochondrial metabolism with photosynthetic carbon assimilation. *Trends in Plant Science* **8**: 546–553.

Raghavendra AS, Padmasree K, Saradadevi K. 1994. Interdependence of photosynthesis and respiration in plant cells: interactions between chloroplasts and mitochondria. *Plant Science* **97**: 1–14.

Rasmusson AG, Soole KL, Elthon TE. 2004. Alternative NAD(P)H dehydrogenases of plant mitochondria. *Annual Review of Plant Biology* **55**: 23–39.

Rhoads DM, Subbaiah CC. 2007. Mitochondrial retrograde regulation in plants. *Mitochondrion* **7**: 177–194.

Sagi M, Fluhr R. 2006. Production of reactive oxygen species by plant NADPH oxidases. *Plant Physiology* **141**: 336–340.

Scheibe R. 2004. Malate valves to balance cellular energy supply. *Physiologia Plantarum* **120**: 21–26.

Scheibe R, Backhausen JE, Emmerlich V, Holtgrefe S. 2005. Strategies to maintain redox homeostasis during photosynthesis under changing conditions. *Journal of Experimental Botany* **56**: 1481–1489.

Shikanai T. 2007. Cyclic electron transport around photosystem I: genetic approaches. *Annual Review of Plant Biology* **58**: 199–217.

Shikanai T. 2014. Central role of cyclic electron transport around photosystem I in the regulation of photosynthesis. *Current Opinion in Biotechnology* **26**: 25–30.

Siedow JN, Umbach AL. 2000. The mitochondrial cyanide-resistant oxidase: structural conservation amid regulatory diversity. *Biochimica et Biophysica Acta*, **1459**: 432–439.

Smirnoff N. 2000. Ascorbic acid: metabolism and functions of a multi-facetted molecule. *Current Opinion in Plant Biology* **3**: 229–235.

Smirnoff N, Wheeler GL. 2000. Ascorbic acid in plants: biosynthesis and function. *Critical Reviews in Biochemistry and Molecular Biology* **35**: 291–314.

Strodtkötter I, Padmasree K, Dinakar C, *et al.* 2009. Induction of the AOX1D isoform of alternative oxidase in *A thaliana* T-DNA insertion lines lacking isoform AOX1A is insufficient to optimize photosynthesis when treated with antimycin A. *Molecular Plant* **2**: 284–297.

Suzuki N, Koussevitzky S, Mittler R, Miller G. 2012. ROS and redox signalling in the response of plants to abiotic stress. *Plant Cell Environment* **35**: 259–270.

Sweetlove LJ, Lytovchenko A, Morgan M, *et al.* 2006. Mitochondrial uncoupling protein is required for efficient photosynthesis. *Proceedings of the National Academy of Sciences U S A* **103**: 19587–19592.

Taira Y, Okegawa Y, Sugimoto K, Abe M, Miyoshi H, Shikanai T. 2013. Antimycin A-like molecules inhibit cyclic electron transport around photosystem I in ruptured chloroplasts. *FEBS Open Biology* **3**: 406–410.

Tan YF, O'Toole N, Taylor NL, Millar AH. 2010. Divalent metal ions in plant mitochondria and their role in interactions with proteins and oxidative stress-induced damage to respiratory function. *Plant Physiology* **152**: 747–761.

Tosti N, Pasqualini S, Borgogni A, *et al.* 2006. Gene expression profiles of O_3-treated Arabidopsis plants. *Plant Cell Environment* **29**: 1686–702.

Tóth SZ, Schansker G, Garab G. 2013. The physiological roles and metabolism of ascorbate in chloroplasts. *Physiologia Plantarum* **148**: 161–175.

Van Aken O, Giraud E, Clifton R, Whelan J. 2009. Alternative oxidase: a target and regulator of stress responses. *Physiologia Plantarum* **137**: 354–361.

Vanlerberghe GC. 2013. Alternative oxidase: a mitochondrial respiratory pathway to maintain metabolic and signaling homeostasis during abiotic and biotic stress in plants. *International Journal of Molecular Science* **14**: 6805–6847.

Vassileva V, Simova-Stoilova L, Demirevska K, Feller U. 2009. Variety-specific response of wheat (*Triticum aestivum* L.) leaf mitochondria to drought stress. *Journal of Plant Research* **122**: 445–454.

Velikova V, Yordanov I, Edreva A. 2000. Oxidative stress and some antioxidant systems in acid rain-treated bean plants: protective role of exogenous polyamines. *Plant Science* **151**: 59–66.

Vishwakarma A, Bashyam L, Senthilkumaran B, Scheibe R, Padmasree K. 2014. Physiological role of AOX1a in photosynthesis and maintenance of cellular redox homeostasis under high light in *Arabidopsis thaliana*. *Plant Physiology and Biochemistry* **81**: 44–53.

Voss I, Sunil B, Scheibe R, Raghavendra AS. 2013. Emerging concept for the role of photorespiration as an important part of abiotic stress response. *Plant Biology* **15**: 713–722.

Wagner AM, Krab K, Wagner MJ, Moore AL. 2008. Regulation of thermogenesis in flowering Araceae: the role of the alternative oxidase. *Biochimica et Biophysica Acta* **1777**: 993–1000.

Walker D, Walker R. 1987. *The use of the oxygen electrode and fluorescence probes in simple measurements of photosynthesis*. Sheffield: University of Sheffield Press.

Wang H, Liang X, Huang J, *et al.* 2010. Involvement of ethylene and hydrogen peroxide in induction of alternative respiratory pathway in salt-treated Arabidopsis calluses. *Plant Cell Physiology* **51**: 1754–1765.

Wang J, Rajakulendran N, Amirsadeghi S, Vanlerberghe GC. 2011. Impact of mitochondrial alternative oxidase expression on the response of *Nicotiana tabacum* to cold temperature. *Physiologia Plantarum* **142**: 339–351.

Weber AP, Linka N. 2011. Connecting the plastid: transporters of the plastid envelope and their role in linking plastidial with cytosolic metabolism. *Annual Review of Plant Biology* **62**: 53–77.

Xia D, Yu CA, Kim H, *et al.* 1997. Crystal structure of the cytochrome bc1 complex from bovine heart mitochondria. *Science* **277**: 60–66.

Xu F, Yuan S, Lin HH. 2011. Response of mitochondrial alternative oxidase (AOX) to light signals. *Plant Signaling and Behavior* **6**: 55–58.

Yabuta Y, Mieda T, Rapolu M, *et al.* 2007. Light regulation of ascorbate biosynthesis is dependent on the photosynthetic electron transport chain but independent of sugars in Arabidopsis. *Journal of Experimental Botany* **58**: 2661–2671.

Yeremenko N, Jeanjean R, Prommeenate P, *et al.* 2005. Open reading frame ssr2016 is required for antimycin A-sensitive photosystem I-driven cyclic electron flow in the cyanobacterium Synechocystis sp. PCC 6803. *Plant Cell Physiology* **46**: 1433–1436.

Yoshida K, Terashima I, Noguchi K. 2006. Distinct roles of the cytochrome pathway and alternative oxidase in leaf photosynthesis. *Plant Cell Physiology* **47**: 22–31.

Yoshida K, Terashima I, Noguchi K. 2007. Up-regulation of mitochondrial alternative oxidase concomitant with chloroplast over-reduction by excess light. *Plant Cell Physiology* **48**: 606–614.

Yoshida K, Watanabe C, Kato Y, Sakamoto W, Noguchi K. 2008. Influence of chloroplastic photo-oxidative stress on mitochondrial alternative oxidase capacity and respiratory properties: a case study with Arabidopsis yellow variegated 2. *Plant Cell Physiology* **49**: 592–603.

Yoshida K, Watanabe CK, Hachiya T, *et al.* 2011a. Distinct responses of the mitochondrial respiratory chain to long- and short-term high-light environments in *Arabidopsis thaliana*. *Plant Cell Environment* **34**: 618–628.

Yoshida K, Watanabe CK, Terashima I, Noguchi K. 2011b. Physiological impact of mitochondrial alternative oxidase on photosynthesis and growth in *Arabidopsis thaliana*. *Plant Cell Environment* **34**: 1890–1899.

Zhang DW, Xu F, Zhang ZW, *et al.* 2010. Effects of light on cyanide-resistant respiration and alternative oxidase function in Arabidopsis seedlings. *Plant Cell Environment* **33**: 2121–2131.

Zhang DW, Yuan S, Xu F, *et al.* 2014. Light intensity affects chlorophyll synthesis during greening process by metabolite signal from mitochondrial alternative oxidase in Arabidopsis. *Plant Cell Environment* doi: 10.1111/pce.12438.

Zhang LT, Zhang ZS, Gao HY, *et al.* 2011. Mitochondrial alternative oxidase pathway protects plants against photoinhibition by alleviating inhibition of the repair of photodamaged PSII through preventing formation of reactive oxygen species in Rumex K-1 leaves. *Physiologia Plantarum* **143**: 396–407.

Zhang L-T, Zhang Z-S, Gao H-Y, *et al.* 2012. The mitochondrial alternative oxidase pathway protects the photosynthetic apparatus against photodamage in Rumex K-1 leaves. *BMC Plant Biology* **12**: 40.